ARMA/USRMS 06-957

Spatial relationships between discontinuity orientation and system behavior in underground excavations

Button, E.A.
Department Earth Sciences, ETH-Zurich,, Zurich, Switzerland
Leitner, R., Poetsch, M. and Schubert W. *Graz University of Technology, Institute for Rock Mechanics and Tunneling, Graz, Austria*

ABSTRACT: The discontinuity orientation in foliated or schistose rocks plays a key role in the rock mass response to the excavation process. In projects where stress induced failure is likely this influencing parameter should be considered while evaluating the rock mass behavior. For each general rock mass structure there is a characteristic deformation behavior, changes in rock mass quality will increase displacements, while secondary structures influence both the displacement magnitudes and patterns. Two dimensional simulations are able to capture many behaviors, while 3-D simulations utilizing the ubiquitous joint model can capture some of the trends observed for characteristics rock mass structures; however they appear limited in modeling more complex rock mass geometries.

1. INTRODUCTION

Estimating the rock mass behavior induced during underground engineering activities is the key to developing a successful design. As a basic principle it is necessary to understand the interactions between the existing state of the ground and the perturbations required for completing the project. While this may appear as common sense, the application of this principal may not be straight forward. The response of the ground to the excavation involves multiple processes that interact through path dependent superposition. The impact of this statement is multifold. Not only must we be able to understand the complex behavior of a given ground mass, but we must also be able to simplify it into a geotechnical model. This model provides a basis for the design of the structure and the interpretation of the measurements acquired during construction. To finalize this process we must also consider the complex interaction between the excavation process, the ground, and the installed support.

Over the last 50 years considerable experience has been gained through the failures and successes of the numerous projects constructed throughout the world. This information is often communicated to both researchers and practitioners through symposia, conferences and publications. One of the most influential outcomes of these communications for tunneling was the rock mass classification methods proposed in the early 1970s. Over the last 30+ years these methods have been widely used, modified, extended, as well as questioned. [1,2,3,4,5,6]. Recently there has been a push to take a more direct engineering approach to rock mass characterization and underground excavation design [7,8,9].

Rock mass classification schemes are an attempt to simplify the rock mass-excavation-support interaction into a minimal number of universal parameters that provide a general relationship between the rock mass quality and typical support intensities. What these systems do not communicate is the expected rock mass behavior based on the mechanical response of the given ground mass.

Therefore, when situations are encountered where these systems fail to correlate the rock mass quality with the actual behavior, problems may arise resulting in cost and time overruns.

Over the past 20 years geodetic measurement systems have overtaken conventional convergence tape measurements as the standard for measuring tunnel displacements. This improvement from scalar values to 3-D displacement vectors has provided a much better picture of characteristic tunnel behavior in different rock types. One such rock type for which significant knowledge has been obtained for over the last 15 years is phyllite and other foliated and schistose rocks.

The behaviors of foliated and schistose rock types do not tend to correspond with the results of the various rock mass classification schemes. There are two fundamental characteristics that result in this observation. First, these rocks are inherently anisotropic, therefore the assumption that increased scale and thus fracture density results in a quasi-isotropic response is invalid. We therefore must consider the influence of the anisotropy's relative orientation to the excavation. While this parameter was considered by Wickham [10] for the Rock Structure Rating and incorporated within the RMR-system [1], the maximum rating adjustment amounts to one rock mass class and thus does not seem applicable based on observations. Secondly, the mobilized strength of these types of rocks is also dependent on direction; therefore we must expect non-homogeneous deformations resulting from different failure modes at different locations in the excavated section.

To identify potential failures modes it is necessary to evaluate the influence of the different rock mass structures and strength characteristics on the rock mass behavior and its interaction with the excavation process and support methods, hereby referred to as the system behavior. In this paper we aim to demonstrate the influence of the rock mass structure and quality on observed displacement characteristics (system behavior) and discuss the applicability of various numerical modeling approaches that are valid for these types of rock.

2. BEHAVIOR TYPES

Utilizing site data from several different tunnels constructed over the past 20 years in phyllitic rocks has allowed basic behavior characteristics to be identified. It is acknowledged that a limited selection of case histories can not cover all possible situations; however the variability and similarities in the observations lead to some generalizations.

2.1. Rock Mass Characterization

The characterization of phyllitic and schistose rock masses for tunneling has been discussed by Button [10,12,13] and will be briefly summarized here. Unlike discontinuities formed through brittle processes (fractures, joints, faults); foliation or schistosity planes form through ductile deformation processes which create highly persistent structures throughout the rock unit which may still possess a significant tensile strength. Figure 1 shows an example of this type of rock mass observed during an excavation in the Austrian Alps. Depending on the diagentic and tectonic history of the rock unit, these planes may be extremely planar (e.g. slate) or may be anastomosing about an average orientation (e.g. schist). This slight difference in the foliation type influences the anisotropic response of the rock mass. Folding at multiple scales is commonly found in these rock types and can result in highly heterogeneous behavior distributions, but will not be specifically discussed in this contribution.

A planar foliation will be highly persistent in a single plane and in order for a crack to develop between adjacent planes the fracture must propagate through the "intact" material. An anastomosing foliation will, on the other hand, have weak planes which cross the apparent anisotropy resulting in a multitude of orientations in which the weak planes forming the foliation are continuous. This allows a fracture to develop across the average anisotropy plane with relative ease.

Fig. 1. Typical geological conditions in a foliated rock mass observed at the tunnel face, corresponds with Fig. 2.

While this influence is not specifically discussed in the published literature, Rumarmurthy and co-

workers [14,15,16] discuss the different characteristic shapes of Uniaxial Compressive Strength versus orientation for phyllitc rocks of the Himalaya. The shape of the curve may follow that for the single plane of weakness theory ("U-Shaped"), or it may be more complex showing a "shoulder-shape" or a "W–shape". Unfortunately, while these are some of the most complete published works for this rock type their description of the intact rock and the resulting failure characteristics are not well discussed. We interpret these variations in the anisotropy diagrams to be related to the intact rock texture as observed in our laboratory.

When characterizing the strength of these rock types in the laboratory it is necessary to relate the failure characteristics to the local rock texture [12]. In this manner, variations in measured strength or deformability between different samples can be related to different sample structures. While this does not provide a straight forward correlation between laboratory values and "Rock Mass" properties it allows the basic mechanisms of the failure process to be identified and these processes can then be scaled, based on the rock mass structure, to assist in predicting and interpreting the tunnel behavior.

2.2. Basic Behavior Characteristics

There are two ways of looking at the behavior characteristics of a single cross section in a tunnel. The most convenient method for observing the relationship between the rock mass structure and the behavior is using displacement vector plots with the encountered geological condition overlaid. This allows a direct correlation with the encountered conditions. The second method is to look at the development of each displacement vector with time or the excavation position. These plots show the stabilization characteristics of each monitoring location.

A typical displacement pattern for a tunnel with the foliation dipping at 70° to the left at an angle of approximately 20° counterclockwise to the tunnel axis is shown in Figure 2. An isolated joint cuts through this section but does not influence the deformation characteristics. In this situation the largest displacements occur in the zone tangent to the foliation, while the smallest deformations occur where the foliation intersects the excavation at high angles. We interpret this behavior to result primarily from dilation normal to the foliation surface (axial splitting). If we assume a nearly vertical maximum stress as was probably the case in this example, in this zone the confining pressure is highly reduced at the boundary, while the circumferential stress is

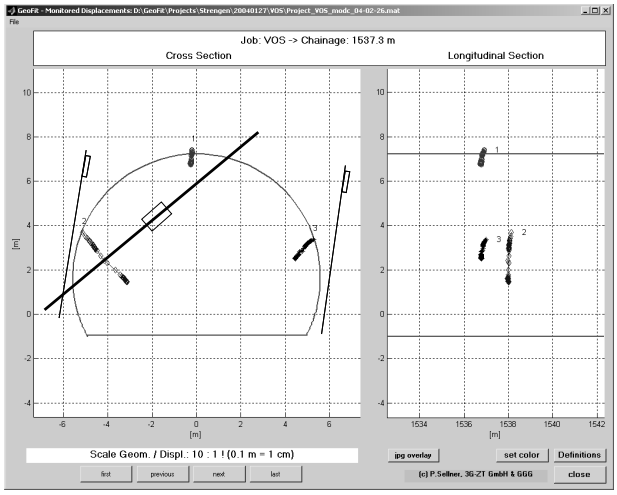

Fig 2. Characteristic displacement pattern for a steeply dipping foliation striking approximately 20° from the tunnel axis. Displacements are at a scale of 10:1 with the excavation.

at a maximum resulting in a nearly uniaxial loading condition, once dialation starts there is continued shearing on the foliation surfaces. This interpretation is supported by simple numerical analyses using the program U.D.E.C. [17] as demonstrated by [18]. Figure 3 shows the results for a single discontinuity dipping at 60°, no support is investigated.

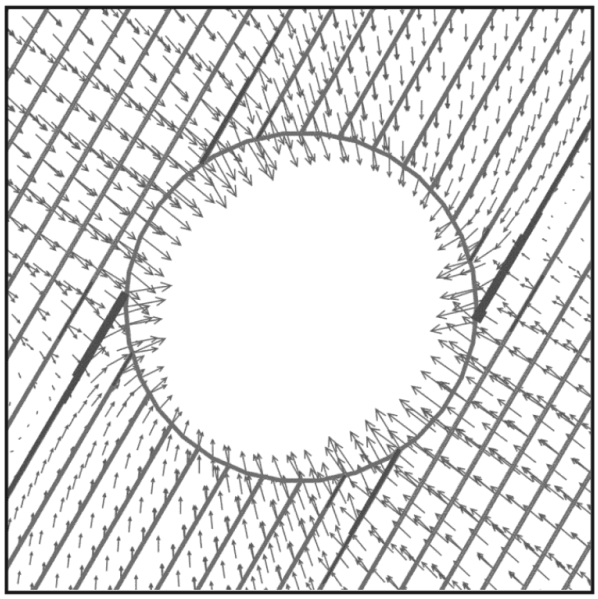

Fig. 3. Displacement vectors associated with a steeply dipping foliation with the maximum stress in the vertical direction [18].

It can be seen that the dominant deformation mechanism is opening between the layers except for the locations where the foliation is almost tangent to the boundary in these zones shearing along the foliation takes place. Joint closure occurs in the region where the foliation is nearly normal to the excavation boundary. The slight difference in the crown measurement between the measured and calculated displacements is most likely due to the installed support (shotcrete and rock bolts) which suppresses the lateral movements of the crown.

This work was extended by [19] who showed the relationship between discontinuity spacing and displacement magnitudes associated with the different deformation modes. Figure 4 shows this influence for the crown, and sidewalls, as well as the minimum and maximum displacements in the cross section.

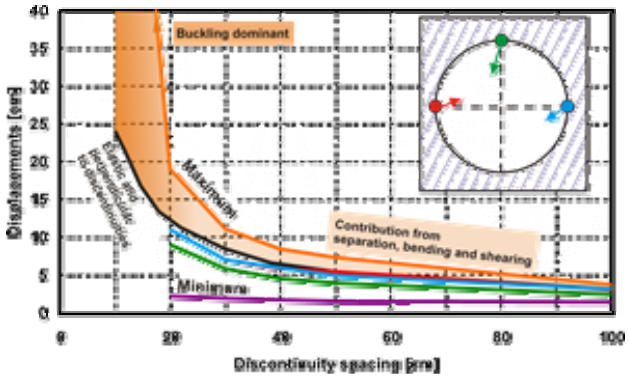

Fig. 4. Relationship between the maximum and minimum displacements for different joint spacing with a dip of 60°, after [19].

It is important to notice in Figure 4 that as the effective spacing decreases the displacement magnitude becomes highly anisotropic and optimal support methods should be tailored to this behavior. Button [12] discussed the characteristic ratio between the crown and sidewall measurement point where the foliation was tangent to the excavation boundary. This value averaged 0.45 with a standard deviation of 0.3. While the ratio between the two sidewall points (tangent to dipping into the tunnel profile) for this typical situation was 1.75 with a standard deviation of 1. The largest variability was associated with low to medium stress levels where singular faults influence the deformations. Thus, the behavior in these cases is not dominated by the general rock structure but by the influence of the singular structures on the stress redistribution and failure kinematics.

In contrast to the discontinuities dipping at acute angles to the maximum principal stress (which is in this case is vertical) where the largest displacements occur in the springline to sidewall regions and highly anisotropic displacement may occur, with a flat dipping foliation the maximum displacements occur in the crown region. Figure 5 shows a measurement section in a good quality rock mass where the foliation dips at approximately 20° in the direction of the excavation striking at nearly 290° from the tunnel axis. The foliation is indicated with the thin black lines and Mueller Flags. It was shown by [12] that for this general situation that the displacement ratio between the crown and the sidewalls was typically between 1.5 and 2 and increased considerably in regions affected by faulting.

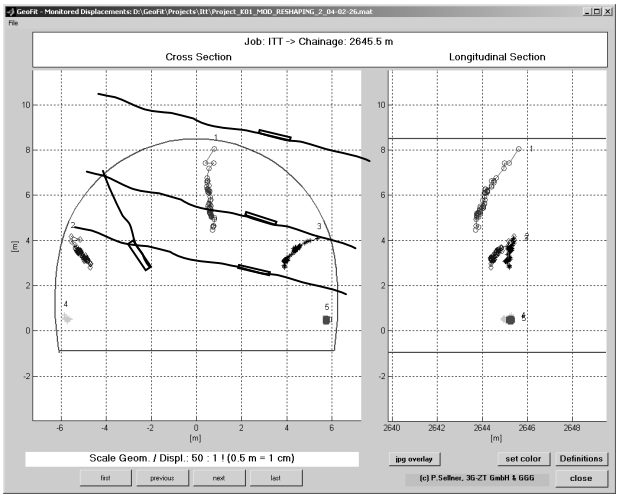

Fig. 5. Displacement characteristics for a flatly dipping foliation. The displacements are at a scale of 50:1 with the excavation [12].

It can been seen in Figure 5 that the displacements measured at both side walls have a similar magnitude and trend while the crown point has a considerably larger displacement. In this section the high longitudinal displacements are indicative of an upcoming fault zone as discussed by [20], [21]. Figure 6 shows the displacement vectors calculated for a dip angle of 30°. For this simulation the results do not correspond with the measurements as well as for the steeper foliation. In these simulations the blocks were assigned elastic behavior to isolate the influence of the discontinuities. In the measured data a combination of failure within the rock, displacements associated with the discontinuities, and the installed support influence the displacement characteristics of the excavation.

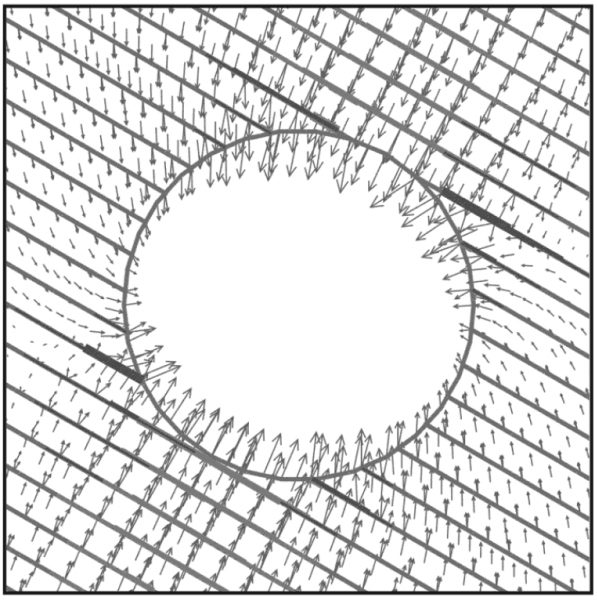

Fig. 6. Calculated displacement vectors for a dip of 30° after [18].

In figure 7 the influence of the rock mass quality on the displacements is demonstrated. In this monitoring section the general rock mass structure was similar to that of figure 5, however a series of foliation parallel faults is located in the upper region of the top heading as schematically shown.

In this situation the general displacement characteristics remain similar to the case with a good rock mass but the displacement magnitudes are approximately 20 times larger. It should also be noted that a ductile support system was used in this region in which gaps were left in the shotcrete lining [22].

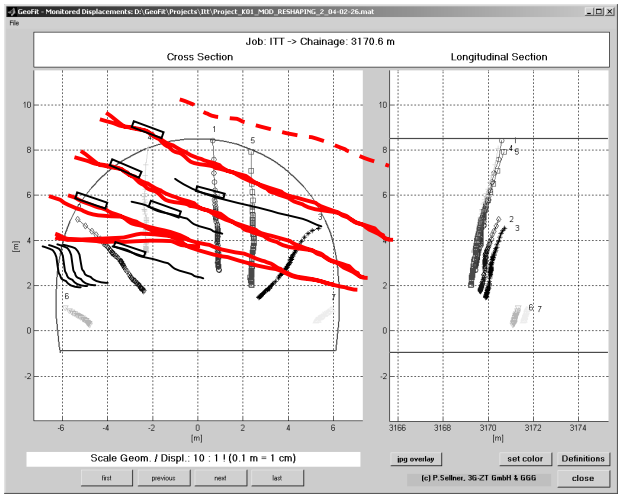

Fig. 7. Displacement vectors associated with multiple foliation parallel faults indicating the influence of decreased rock mass quality on the measured displacements [12].

This support system results in each section of the lining behaving in response to the rock mass behavior directly behind it, which in turn limits the influence of the lining on the anisotropic response of the rock mass, i.e we observe the response much more directly then with a single lining section.

This general trend has been observed regardless of the foliation orientation. The effect of foliation parallel faults is to increase the deformability of the rock mass but the general displacement pattern remains practically unchanged.

The previous examples were in situations were the discontinuities we nearly parallel to the excavation surface (± 20°). The next example discusses a typical response with a steeply dipping foliation that crosses the tunnel axis obliquely (30° to 40°). Figure 8 shows a typical displacement pattern for this situation. A ductile support system was also utilized in this section, however, steel support elements were placed in the lining gaps to improve its load carrying capacity [23]

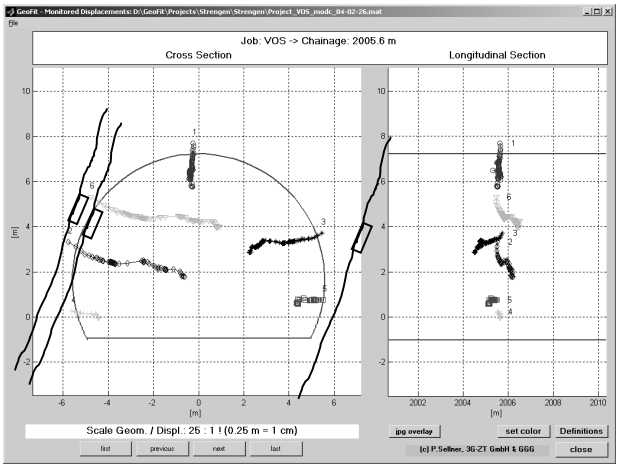

Fig. 8. Displacements associated with an obliquely striking and steeply dipping foliation, modified after [12].

Unlike previous sections shown, two unique characteristics are observable in this plot. The first is the longitudinal displacement characteristics of the side walls which are related to the orientation of the foliation. The points on the left side of the excavation move in the tunnel direction while the point on the right side moves strongly against the tunnel direction. This behavior is interpreted to result from the different kinematic freedoms associated with the displacements on the foliation. On the upper face of the foliation planes (right side) the displacement response results from shearing and opening of the foliations against the direction of the tunnel. On the lower face of the foliation (left side)

the displacements must be in the opposite direction, if sliding were to occur on the upper face it would have to move into the rock mass which is unfeasible. This mechanism is similar to reverse shearing associated with toppling.

The second unique characteristic associated with this displacement plot is the up and down movement of the side wall points. This characteristic behavior has been interpreted and shown to be related to the competing deformation mechanisms between shearing on secondary structures and opening on the main foliation plane. First opening is dominant on the main foliation, as the deformation changes the local stress state shearing on the secondary structures initiates while the opening mode is suppressed. This process then repeats as failure occurs on deeper and deeper planes. Figure 9 shows that this behavior can be simulated using a 2-D simplification by a gradual reduction in the strength of each discontinuity until it begins to fail. The strength of only one discontinuity is decreased at a time until failure and when equilibrium is reached the strength of the next deeper foliation is decreased. This displacement characteristic requires that a secondary texture for example; foliation, discontinuities, excavation induced fractures, etc. crosses the primary structure.

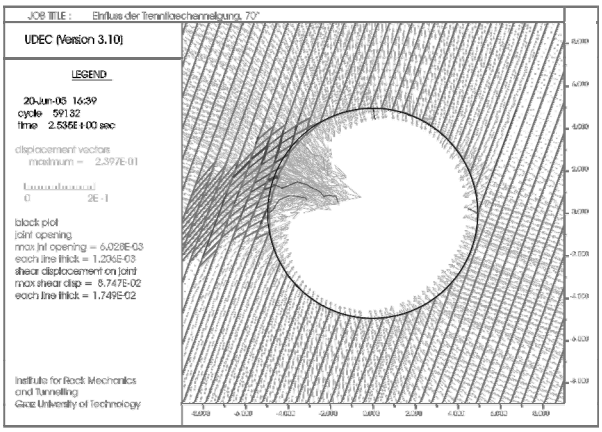

Fig. 9. Variable displacement characteristics associated with multiple failure mechanisms competing as the failure depth increases, the displacement path is highlighted for single points, after [18].

2.3. Complex behavior types

In the previous section the influence of the discontinuity orientation on the displacement characteristics for three examples was shown and discussed. The next section will expand on these basic behavior types to show how non-foliation parallel structures can influence the displacement characteristics.

The first example is from the tunnel discussed above with the steeply dipping foliation. In this section the foliation is striking parallel to the tunnel axis and there are two distinct fault geometries, one fault set is dipping against the tunnel direction at approximately 60° as shown on figures 10 and 11 and a single fault parallel to the foliation that is located a meter or two outside of the excavation. This fault was observed within the tunnel and then exited the excavation area several meters before the first monitoring section. In this section a ductile support system was utilized as described above for this tunnel [23].

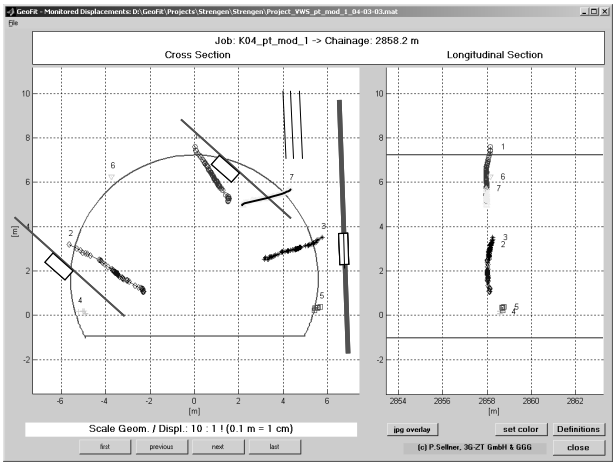

Fig. 10. Displacement characteristics influenced by multiple faults dipping into the excavation and a single fault just outside of the boundary [12].

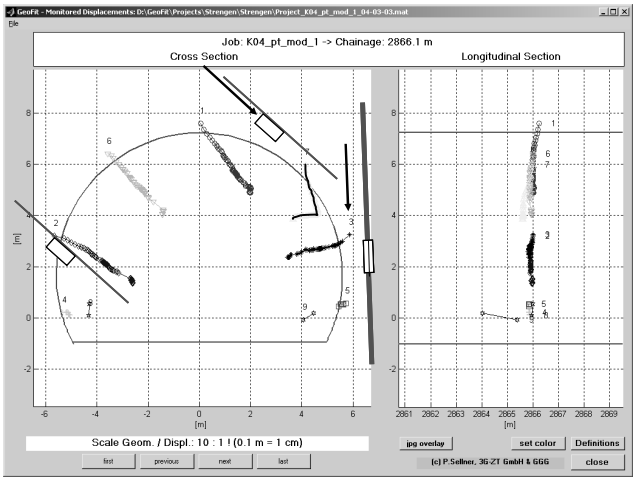

Fig. 11. Displacement characteristics for a change in failure mode related to the position of the faults outside of the excavation [12].

In figure 10 the displacement pattern in the crown and left side wall is dominated by the decreased

rock mass quality and orientation associated with the multiple faults dipping into the excavation, the orientation of the crown point is highly skewed by the fault just above its position. The behavior of the right sidewall points are dominated by the foliation orientation and the fault just outside of the excavation. Both points are located in a single segment of the lining and thus show that the rock mass is basically pushing the lining inwards with the bottom section having a slightly larger displacement.

Figure 11 shows the next monitoring section 8 meters away from that shown in figure 10. In this location the upper fault dipping into the tunnel has completely exited the excavation boundary. Initially the displacements in the left side, the crown and right springline are parallel to the multiple faults, while the right side wall shows a similar behavior to the previous section. After approximately 20 days the springline measurement changes orientation to one similar to the lower sidewall point indicating a change in kinematics associated with shearing dominated by the upper fault to one of shearing and dilatation associated with the foliation parallel fault outside of the boundary.

A second interpretation may also be argued for. In this section the measurement point in the right springline is most likely above the gap in the lining (in the last section it was below this gap). This change in behavior could be the result of the ductile element closing and no longer being able to consume the difference in strain between these two segments. Once the gap is closed the radial stiffness of the upper lining segments increases and the loads are now being transferred though more of the lining and due to the kinematics associated with the ongoing failure in the rock mass the displacement vector changes orientation. Most likely it is a combination of these two scenarios that leads to the observed displacements.

This example also shows the importance of understanding how the support, or small changes in the monitoring point location, can lead to changes in the displacement characteristics. If these changes are misinterpreted then there is a potential for making wrong decisions concerning the excavation and support methods, especially if using advanced data evaluation techniques for estimating the upcoming rock mass conditions [21].

The next example also deals with a fault zone near the excavation boundary, however in this case the fault is not parallel with the foliation. This example is from the tunnel with a relatively flat foliation discussed above. Figure 12 shows a monitoring section with the fault zone located in the right-central section of the excavation. Several foliation parallel faults also influence the behavior resulting in a displacement pattern similar to that shown in figure 7. The maximum displacement is in the crown while the right springline deforms more then the left showing the local influence of the fault. The two side wall points show a similar trend with the right side displacing slightly more than the left.

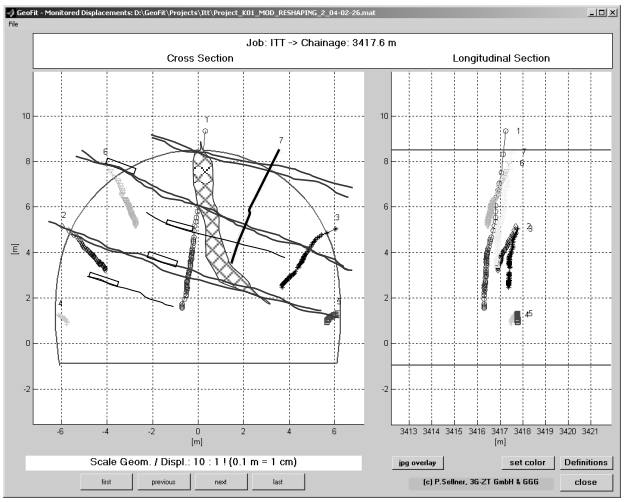

Fig. 12. Displacement characteristics influence by foliation parallel faulting and a foliation normal fault in the center of the excavation.

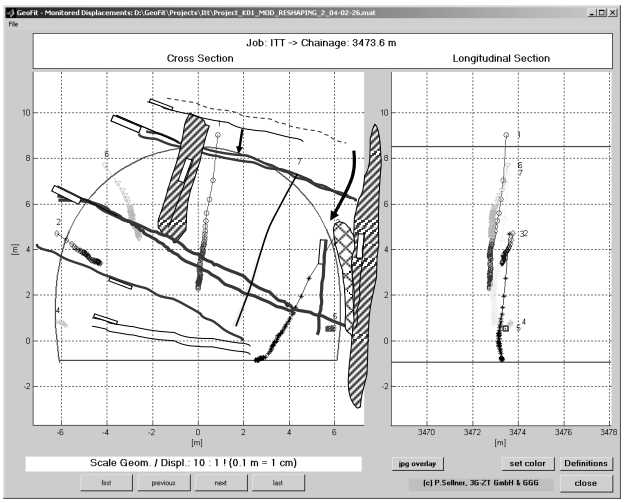

Fig. 13. Displacement characteristics influenced by foliation parallel and foliation normal faulting outside of the excavation profile [12].

Figure 13 shows a cross section approximately 55 m after the section shown in figure 12, in which the

fault has increased in size and migrated outside of the excavation profile. In this section the displacement of the lower right side wall point has the largest magnitude while the displacements on the left side of the excavation have now decreased to levels observed before this structure was encountered. We interpret this displacement pattern as being dominated by failure of the pillar between the steep fault and the excavation resulting in shearing along the steep fault. This causes the entire right side of the excavation to move downwards and rotate slightly into the excavation. The basic geological conditions are quite similar to that shown in figure 7, however in this case the influence of the second fault geometry is superimposed on the typical response associated with only a foliation parallel fault system.

The two examples have both shown that displacements increase when a fault is located just outside of the excavation surface. This failure process (overstressing of the pillar) may lead to different displacement characteristics but will usually result in anisotropic and heterogeneous deformations as the area influenced by this process is limited by the geometry of the system and can be local or over considerable distances. It is necessary to respond quickly to these changes in order to prevent this type of situation from getting out of control.

3. SIMULATING BEHAVIOR TYPES

In order to provide a prediction during design or to evaluate specific problems during construction; it is often necessary to perform numerical simulations to evaluate different failure modes and remedial measures for the expected conditions. The choice of which type of code and at which detail should the model represent the actual or expected conditions is often a balance between information, time, and resources. In the previous discussion 2-D distinct element analyses where used to show how the spatial characteristics of the discontinuities relative to the maximum principal stress influenced the deformation modes. With increasing computing power it is becoming possible to run 3-D codes in a reasonable time, and therefore they are being used more frequently. To simulate foliated rock mass one must make a decision regarding the type of analyses to be used. For this rock type there are three general possibilities:

- Continuum code with anisotropic elastic properties
- Continuum code with an anisotropic failure criteria
- Discontinuum code

Depending on the expected behavior, each of these possibilities has distinct benefits and drawbacks. In this work we would like to show that general characteristics of the observed behavior can be captured within 3-D continuum models though there are limitations to capturing more complex behavior modes.

3.1. Review

Over the past 25 years there have been several publications or dissertations that have investigated the influence of anisotropy on tunnel behavior in 3-D simulations. Wittke [24] presented the results of 3-D anisotropic simulations for four cases utilizing elastic material behavior for a shallow tunnel. These simulations showed that there was a strong influence on the resulting displacement vectors, with the largest displacements occurring for a horizontal anisotropy plane and the smallest displacements occurred for a vertical plane normal to the tunnel axis. Tonon [25] in his dissertation implemented anisotropic elastic behavior in the 3-D finite-element – boundary element code B.E.F.E. [26] and reported results concerning the use of advanced data evaluation methods [21] for identifying changes in rock mass quality ahead of the face in anisotropic material as well as the effect of the anisotropy on lining loads.

3.2. Modeling Results

In this work we have utilized the commercial code F.L.A.C. [27] to simulate the behavior of a 10 m diameter circular tunnel utilizing the ubiquitous joint model to capture the anisotropic failure behavior associated with foliated rock types. The overburden was assumed to be 600 m and k_0 was 0.7. The implemented material properties were those utilized by [18,19]. The model is a 100 m long and 200 m in both the vertical and horizontal directions. No support was used in the simulation so only the response of the rock mass structure is considered. For this contribution the displacement behavior characteristics of four simulations will be discussed. The results are shown for a cross section located in the middle of the model (station 50).

In order to allow a general comparison between measured data and simulation results the zero reading is taken in this case to be the end of the previous excavation step. This measurement is placed on the tunnel boundary; displacements outside of the tunnel are pre-displacements while displacements displayed in the tunnel are potentially measurable with standard geodetic measurements. The displacements are displayed with at ratio of 10:1 with the excavation geometry.

The first simulation (Case 1) considered a standard case where the plane of anisotropy was normal to the tunnel axis and dipping at 90°. Figure 14 shows both the cross sectional and longitudinal distribution of the displacements at 12 locations distributed around the tunnel. In this case the largest displacement is 104 mm (33 mm measured) and located in the crown. The longitudinal displacements in this case are practically zero indicating that the deformations are confined to shearing within the anisotropic planes and very little joint opening is captured at the excavation boundary.

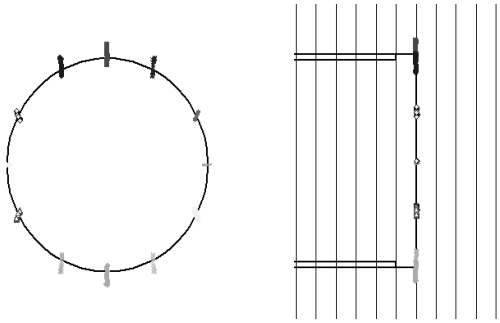

Fig. 14. Displacements associated with a vertical foliation striking perpendicular to the tunnel axis.

Figure 15 shows the results for a simulation with the plane of anisotropy striking parallel to the tunnel axis and dipping at 90° (Case 2). The maximum displacements were at the side walls and had a magnitude of 1539 mm (1534 measured). The crown displacements were approximately 175 mm (145 measured). This is a increase of 15 times compared with the Case 1 normal to the tunnel axis With this case the pre-displacements at the side wall were minimal and increased in magnitude towards the crown or invert.

The longitudinal displacements in this case show an interesting pattern that assists in interpreting the results. All of the points displace slightly in the tunneling direction with the largest longitudinal displacements occurring at the side walls decreasing to practically zero at the crown. In this location the magnitude increases gradually with distance to the tunnel face. This is the result of buckling (doming), since the face position limits the initiation of this mechanism. It takes several excavation steps to start occurring, therefore since this monitoring point is between the center of the doming and the face it moves slightly in the direction of the excavation advance. This effect decreases with increasing distance from the location where the foliation is tangent to the excavation boundary.

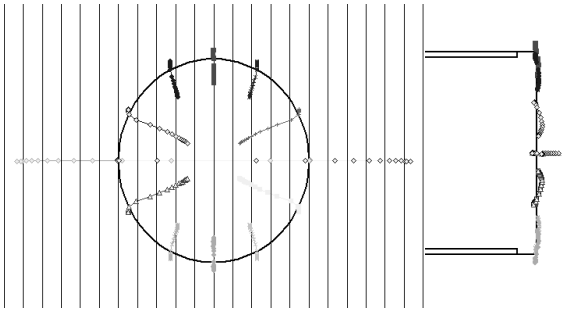

Fig. 15. Displacements associated with a vertical foliation striking parallel to the tunnel axis.

Figure 16 shows the results for Case 3 where the plane of anisotropy is striking 15° from the tunnel axis and the dip is 70°. This case is used to compare the measurements from the tunnel with the steep foliation discussed in Section 2. The maximum displacements were in the upper and lower side walls where the foliation was tangent to the tunnel boundary as expected.

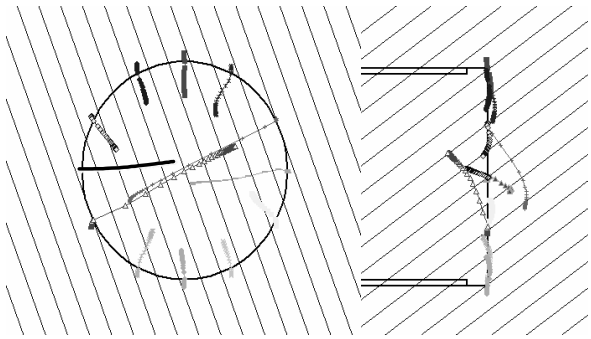

Fig. 16. Displacements associated with a foliation dipping at 70° striking 15° from the tunnel axis.

The maximum displacement was approximately 820 mm (808 measured) with the upper side wall point displacing slightly more than the opposite lower side wall point, most likely due to gravity effects.

The crown displaces approximately 200 mm (150 mm measured).

In this case the longitudinal displacements show a similar trend to those observed in the tunnel, with the points on the right side of the excavation (below the plane) moving in the tunnel direction and those on the left side (above the plane) moving against the tunnel direction. The magnitude of the longitudinal displacement decreases with distance from the location where the foliation is tangent to the excavation. The general displacement trend around the excavation agrees quite well the measured data.

The final simulation geometry (Case 4) was performed to investigate the cases discussed in Section 2 for the tunnel with a relatively flat dipping foliation, figure 17. The plane of anisotropy in this case dips at 25° in the tunnel direction striking at 310° to the tunnel axis. In this case the maximum displacement of 180 mm (measured 150 mm) is at the crown. The upper sidewall points (at a similar location to the monitored points) have a displacement of approximately 40 mm (35 mm measured). The longitudinal displacements in this case show opposite orientations with the crown points moving in the direction of the excavation (above the plane) and the lower points moving slightly against the excavation direction (below the plane). This trend is the same as in Case 3, but not as pronounced as in this case the strike is 40 degrees from the tunnel axis decreasing the kinematic freedom for this displacement mechanism.

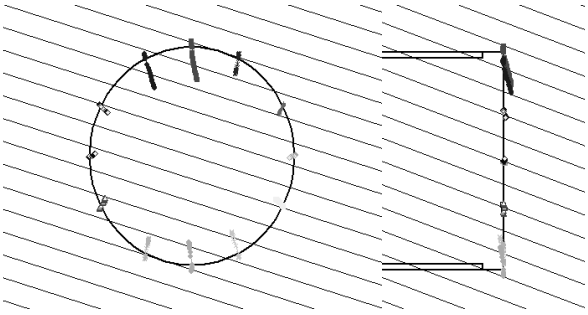

Fig. 17. Displacements associated with a foliation dipping at 25° in the tunnel direction striking at 130° to the tunnel axis.

4. CONCLUSION

In this paper we have demonstrated that the relative orientation between the excavation axis and the foliation (plane of anisotropy) can have a large impact on the rock mass behavior characteristics. This influencing factor must be considered when evaluating which simplifications should be made for designing underground excavations. When the rock mass remains in the elastic behavior range this parameter is less important in relation to the global rock mass deformation characteristics, but must be considered when evaluating the potential for systematic or localized overbreaks and block falls.

When the rock mass begins to fail under the excavation induced stresses, the influence of the anisotropy increases considerably and should be considered when evaluating the potential rock mass behavior types used for design. The use of rock mass classification schemes becomes increasingly risky as the influence of the anisotropy on the rock mass behavior increases.

For situations where the rock mass quality decreases but no secondary structures are present the characteristics displacement pattern remains similar, but the displacement magnitude increases. In cases where secondary structures are present, there is a high probability that not only will displacements increase but their pattern will also change, often over very short sections. This results in heterogeneous displacement distributions which must be considered for optimizing support methods for the encountered conditions. One must also be aware of how the installed support or the measurement locations can influence the results when the excavation does not deform radially.

Simulating the general behavior of anisotropic rock masses shows promising results in 3-D. The method utilized in this discussion (ubiquitous joints) can capture some of the general trends, but may not be suitable for investigating more complex rock mass conditions. Additionally, different displacement mechanisms, such as joint opening or closure, are more difficult to simulate with this model compared to distinct element methods. The extremely large displacements determined for Case 2 were due to buckling of the ubiquitous layers. It is necessary to define an effective layer thickness for these types of rocks if a discrete element simulation is to be used. For the 2-D case with a tunnel radius of 5 m, the system started to buckle at a spacing of less then 20 cm, or at less than 5% of the tunnel radius. To use this type of spacing in a 3-D distinct element code is practically impossible with today's memory limitations (currently 1.012 GB for 3-DEC). Future work must focus on which simplifications and which assumptions can be utilized in 3-D modeling while still capturing the correct mechanisms and

interactions and providing realistic trends and magnitudes in more critical and complex rock mass structures.

References

1. Bieniawski, Z.T. 1974. Geomechanics classification of rock masses and its application in tunnelling. In *Advances in rock mechanics* 2 (A), 27-32. Washington, D.C.: Nat. Acad.Sci.

2. Bieniawski, Z.T. 1989. *Engineering rock mass classifications.* pp 251. New York: Wiley.

3. Barton, N., R. Lien, & J. Lunde, 1974. Engineering classification of rock masses for the design of tunnel support. *Rock Mechanics* 6*:4*: 189-236, Vienna: Springer.

4. Barton, N.. 1998. NMT support concepts for tunnels in weak rocks. In *Proceedings Int. Symp. Tunnels and Metropolises*, eds. A. Negro Jr.and A.A.Fierreira. San Palo: Rotterdam Balkema. 273-279.

5. Riedmüller, G., W. Schubert. 2001. Critical comments on quantitative rock mass classifications. *Felsbau* 17:3 164-167.

6. Palmstron, A., E. Broch. 2006 (in press). Use and misuse of rock mass classification systems with particular reference to the Q-system. *Tunnelling and Underground Space Technology.*

7. Schubert, W., A. Goricki, E.A. Button, G. Riedmueller, P. Poelsler, A. Steindorfer, R. Vaneck. 2001. Excavation and support determination for the design and construction of tunnels. In *Proceedings of the ISRM Regional Symposium Eurock, Rock Mechanics: A Challenge For Society*, *Espoo, Finland*. eds. P.Särkkä and P. Eloranta. 383-388 . Rotterdam: A.A. Balkema

8. Österreichishe Gesellschaft für Geomechanik. 2001. *Richtlinie für Geomechanische Planung von Untertagebauarbeiten mit zyklischem Vortrieb*. ÖGG, Salzburg. pp. 30

9 Kaiser, P.. 2006. Tunnel stability in highly stressed, brittle ground – A rock mechanics approach to deep tunnelling. *In Proc. Geology Alp Transit*. ed. S. Loew. 27-30 Sept. 2005. Zurich, Switzerland. in press.

10. Wickham, G.E., H.R. Tiedemann, E.H. Skinner. 1974. Ground Support Prediction Model, RSR Concept. In. *Proc. Rapid Excav. Tunnelling Conf.* 691-707. AIME, New York.

10. Button, E.A., M. Bluemel. 2004. Characterization of Phyllitic and Schistose rock masses: From System Behaviour to Key Parameters. In *Proceedings of the ISRM Regional Symposion Eurock: Rock Engineering: From Theory to Practice, Salzburg, Austria.* ed. W. Schubert. 459-464.

12. Button, E.A. 2004. *A contribution to the characterization of phyllitic and schistose rock masses for tunnelling*. Doctoral Thesis. Graz University of Technology. pp. 134.

13. Button, E.A. 2004. Characterization of Phyllites for Tunnelling. *Int. J. of Rock Mechanics Min. Sci.* 41, Supplement 1: 215-220

14. Ramamurthy, T. 1993. Strength and Modulus Responses of Anisotropic Rocks. *In Comprehensive Rock Engineering*. ed. J.A. Hudson. 1: 313-329.

15. Ramamurthy, T., K.S. Rao, J. Singh. 1993. Engineering behaviour of phyllites. *Engineering Geology*. 33: 209-225.

16. Nasseri, M.H.B., K.S. Rao, T. Ramamurthy. 2003. Anisotropic strength and deformational behaviour of Himalayan schists. *Int. J. Rock Mech. Min. Sci.* 40:1 3-23.

17. Itasca Consulting Group, Inc.: Universal Distinct Element Code (UDEC). Version 4.0. 2004. Minneapolis, Minnesota

18. Goricki, A., E.A. Button, W. Schubert, M. Pötsch, R. Leitner. 2005. The Influence of Discontinuity Orientation on the Behaviour of Tunnels. *Felsbau* 23:5 12-18.

19. Leitner, R. M. Poetsch, W. Schubert. 2006. Aspects on the numerical modelling of rock mass anisotropy in tunnelling. *Felsbau 2:(in press)*

20. Steindorfer, A.F. 1998. *Short term Prediction of Rock Mass Behaviour in Tunnelling by advanced Analysis of Displacement Monitoring Data*. PhD Thesis, Graz University of Technology, Austria. In *Schriftenreihe der Gruppe Geotechnik Graz*, G. Riedmüller, W. Schubert, S. Semprich (eds.). Heft 1. Graz

21. Schubert, W., Steindorfer, A., Button, E.A. (2002); Displacement Monitoring in Tunnels – an Overview. *Felsbau.* 20:2. 7-15.

22. Schubert, W. 1996. Dealing with squeezing conditions in alpine tunnels. *Rock Mechanics and Rock Engineering, 29:3.* 145-153. Wien: Springer.

23. Button, E.A., Schubert, W., Moritz B. 2003. The Application of Ductile Support Methods in Alpine Tunnels. *ISRM 2003–Technology roadmap for rock mechanics*, South African Institute of Mining and Metallurgy. 1: 163 - 166.

24. Wittke, W., 1990. *Rock Mechanics*. Springer-Verlag. Berlin.

25. Tonon, F., 2000. *Three-Dimensional Modelling of Underground Excavations and Estimation of Boundary Conditions in Rock with Fabric*. Doctoral Thesis, Univ. Colorado-Boulder. pp. 396.

26. Beer, G. 1999. Boundary Element-Finite Element Code. (BEFE). Technical University Graz.

27. Itasca Consulting Group, Inc. 2002. Fast Lagrangian Analysis for Continua in three Dimensions (FLAC3D). Version 2.1. Minneapolis, Minnesota